Journal of Sound and Vibration 329 (2010) 3451–3469

Contents lists available at ScienceDirect

Journal of Sound and Vibration

journal homepage: www.elsevier.com/locate/jsvi

Vibration analysis of a partially treated multi-layer beam with magnetorheological fluid

Vasudevan Rajamohan, Subhash Rakheja, Ramin Sedaghati *

CONCAVE Research Centre, Department of Mechanical Engineering, Concordia University, Montreal, Quebec, Canada H3G1M8

ARTICLE INFO

Article history:
Received 10 September 2009
Received in revised form
1 March 2010
Accepted 8 March 2010
Handling Editor: D.J. Wagg
Available online 9 April 2010

ABSTRACT

Semi-active vibration control based on magnetorheological (MR) materials offers excellent potential for high bandwidth control through rapid variations in the rheological properties of the fluid under varying magnetic field. Such fluids may be conveniently applied to partial or more critical components of a large structure to realize more efficient and compact vibration control mechanism with variable damping. This study investigates the properties and vibration responses of a partially treated multi-layer MR fluid beam. The governing equations of a partially treated multi-layered MR beam are formulated using finite element method and Ritz formulation. The validity of the proposed finite element formulations is demonstrated by comparing the results with those obtained from the Ritz formulation and the experimental measurements. The properties of different configurations of a partially treated MR-fluid beam are evaluated to investigate the influences of the location and length of the MR-fluid for different boundary conditions. The properties in terms of natural frequencies and loss factors corresponding to various modes are evaluated under different magnetic field intensities and compared with those of the fully treated beams. The effect of location of the fluid treatment on deflection mode shapes is also investigated. The forced vibration responses of the various configurations of partially treated MR sandwich beam are also evaluated under harmonic force excitations. The results suggest that the natural frequencies and transverse displacement response of the partially treated MR beams are strongly influenced not only by the intensity of the applied magnetic field, but also by the location and the length of the fluid pocket. The application of partial treatment could also alter the deflection pattern of the beam, particularly the location of the peak deflection.

1. Introduction

Active vibration control systems are known to yield enhanced vibration suppression of structures and adapt to changes in the excitation and structural properties [1–3]. The applications of such systems, however, could be justified in situations where the high cost and large power requirements outweigh the performance gains. Alternatively, semi-active damping control could yield the performance advantages similar to those of an active control device with only minimal power requirement [4–6]. Fluids with controllable rheological properties, such as electrorheological (ER) and magnetorheological (MR) fluids, are increasingly being used as semi-active vibration devices in various applications such as automotive

* Corresponding author. Tel.: +1 514 848 2424x7971; fax: +1 514 848 3175.
E-mail addresses: v_rajamo@encs.concordia.ca (V. Rajamohan), rakheja@alcor.concordia.ca (S. Rakheja), sedagha@encs.concordia.ca (R. Sedaghati).

0022-460X/$ - see front matter © 2010 Elsevier Ltd. All rights reserved.
doi:10.1016/j.jsv.2010.03.010

suspensions and structures [7–9]. Such fluids can provide significant and rapid changes in the damping and stiffness properties with application of an electric or magnetic field [10]. Although these have been widely presented as smart controllable fluids, the ER fluids exhibit a number of shortcomings compared to the MR fluids such as low yield strength, requirement of high voltage and greater sensitivity to common impurities [11]. The MR fluid, on the other hand, exhibits yield stress in the order of 2–3 kPa range in the absence of an external magnetic field which rapidly exceeds 80 kPa in the presence of a magnetic field in the order of 3000 Oe [12]. The MR fluid is also known to be well-suited for high bandwidth control through rapid variations in its rheological properties under a varying magnetic field.

The properties of ER and MR-fluid dampers have been widely characterized analytically and experimentally for vibration suppression of structures and systems [9,13,14]. The application and potential benefits of controllable ER and MR damping devices have been explored in a number of studies employing simple structure models [15,16]. These models employ lumped ER/MR dampers at selected discrete locations of the structure and require multiple damping elements to control the vibration corresponding to different modes. The ER/MR fluids have also been implemented to achieve controllable distributed properties in structures comprising embedded ER/MR material layers between two elastic/metal layers [17–21]. This approach can facilitate control of structure vibration over a broad range of frequencies through variations in distributed stiffness and damping properties in response to applied electric or magnetic field.

While a number of studies have analyzed sandwich structures with ER fluids [17–20], the application of MR materials in sandwich structures have been explored in a very few studies. Yalcintas and Dai [21,22] analyzed the dynamic responses of a MR fluid adaptive structure using the analytical energy approach and compared the responses with those of the structure employing ER-fluid. It was concluded that MR fluid based adaptive structure can yield significantly higher natural frequencies, nearly twice that of the ER fluid based adaptive structure. Sun et al. [23] investigated the dynamic response of a MR sandwich beam analytically using energy approach and compared the results with the experimental results. Experiments were also performed to estimate the relationship between the applied magnetic field and the complex shear modulus of the MR fluid using oscillatory rheometry technique. Yeh and Shih [24] analyzed the dynamic characteristics and instability of MR adaptive structures based on DiTaranto [25] sixth-order partial differential equation together with incremental harmonic balance method. Rajamohan et al. [26] investigated the dynamic properties of a MR sandwich beam using finite element and Ritz formulations and compared the results using the experimental investigations. A free oscillation experiment was also performed to estimate the complex shear modulus of the MR fluid. The above studies have considered fully treated beam structures with ER/MR fluid layer over the entire beam length. Alternatively, such fluids may be applied over the partial beam lengths or more critical section of a large structure to achieve more efficient and compact vibration control mechanism. Haiqing et al. [27] experimentally analyzed the vibration characteristics of a cantilever beam locally linked by ER fluid layer to the ground. It was concluded that the locally applied ER fluid layer serves as a complex spring and thus alters the damping and stiffness properties of the structures under the electric field. The study also concluded that the cantilever beam with such local treatment exhibits greater sensitive than the full treatment with regards to the natural frequencies and loss factors. Haiqing and King [28] investigated the vibration response of a fully and partially treated ER beam clamped at both ends and concluded that the length of the ER fluid layer has a significant effect on the resonant frequencies and the loss factor. The effectiveness of partial treatment of MR fluids in sandwich structures, however, has not yet been explored.

In this present study, the governing equation of a partially treated multi-layer MR beam is developed in the finite element form and Ritz formulation. The validity of the proposed finite element formulations is demonstrated by comparing the results with those obtained from the Ritz formulation and laboratory measurements performed on a prototype beam. The effects of lengths and locations of the MR fluid layers on the properties of the beam are investigated under different intensities of the external magnetic field, and various boundary conditions. Furthermore, the properties of the partially treated beams are compared with those of the fully treated MR sandwich beam. Finally, the forced vibration responses of different partially treated MR sandwich beam configurations are evaluated under harmonic force excitations.

2. Dynamic model of a partially treated multi-layer beam

A partially treated sandwich beam structure can be modeled on the basis of those developed for a fully treated beam. The beam structure with multiple MR-fluid segments can be modeled by treating each segment independently and then coupling with the adjacent segments to assure compatible deformation and continuous response of the composite structure. This could be achieved by imposing compatibility conditions which are identical displacements and the slopes at the boundaries of the two adjacent segments. A three-layer beam structure comprising a MR-fluid layer over the entire beam length between two elastic layers, as shown in Fig. 1(a), is considered as the basis for developing the finite element model and Ritz formulation for the partially treated MR sandwich beam shown in Fig. 1(b). The mid-layer of the partially treated sandwich beam is composed of elastic layers of lengths L_1 and L_3 and a MR fluid layer segment of length L_2. Considering that Young's modulus of the MR-fluid is nearly negligible compared to that of the elastic layers, the normal stresses in the fluid layer are considered to be neglected. The elastic and fluid layers thickness, h_1, h_2 and h_3, are considered to be very small compared to the length of the beam. The shear strain and the damping in the elastic layers are also assumed to be negligible. The slippage between the elastic and fluid layers is further assumed to be negligible.

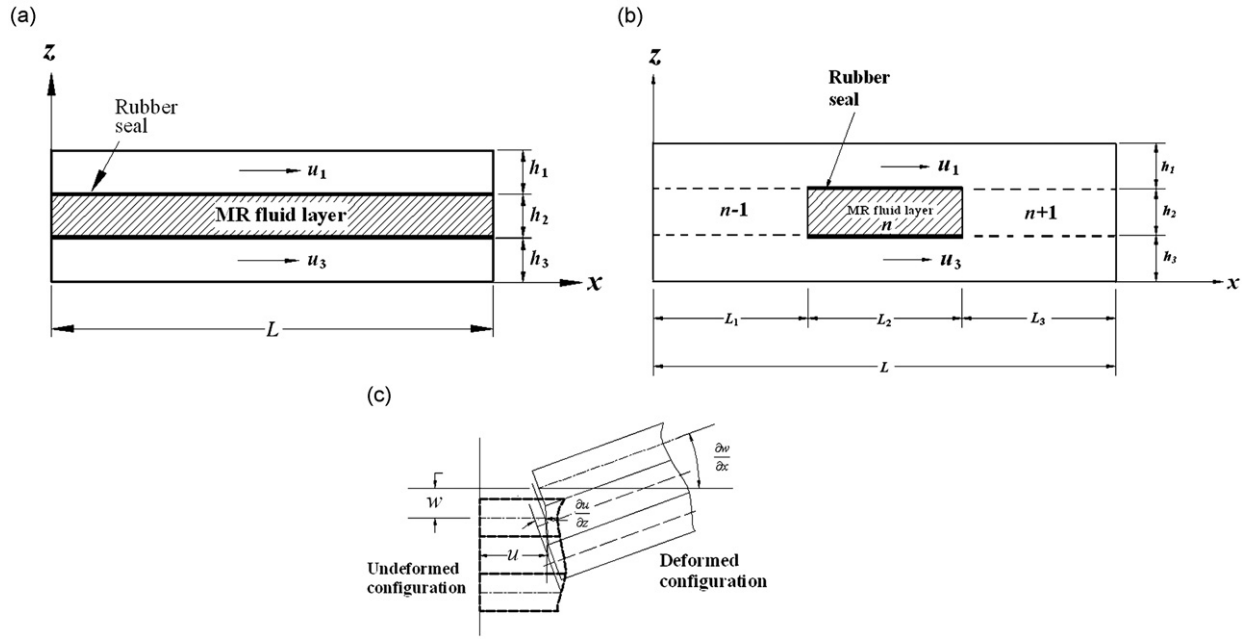

Fig. 1. (a) Fully treated MR sandwich beam, (b) partially treated MR sandwich beam, and (c) deformed and undeformed beam cross section.

Furthermore, the variation of the through the thickness displacement is assumed to be negligible and thus the transverse displacement w is considered to be uniform throughout the given cross section.

Let the longitudinal displacements of the mid-planes of the top, middle and bottom layers in the x-direction be u_1, u and u_3, respectively. As the mid layer is assumed as a neutral layer in the transverse plane, the top and bottom surfaces are considered to experience axial compression and tension, respectively. Consequently, the axial displacement of the sandwich beam is considered to be equivalent to the axial displacement at the mid-layer of the beam. The strains and displacements in the axial and transverse directions are shown in Fig. 1(c). The shear strain γ in the MR layer can be derived from [29]

$$\gamma = \frac{\partial w}{\partial x} + \frac{\partial u}{\partial z} \tag{1}$$

where

$$\frac{\partial u}{\partial z} = \frac{(h_1+h_3)}{2h_2}\,\frac{\partial w}{\partial x} + \frac{(u_1-u_3)}{h_2} \tag{2}$$

and w is the transverse displacement.

That yields shear strain as a function of the layers' thickness as

$$\gamma = \frac{D}{h_2}\,\frac{\partial w}{\partial x} + \frac{u_1-u_3}{h_2} \tag{3}$$

where $D = h_2 + 1/2(h_1+h_3)$.

Let F_1 and F_3 be the longitudinal forces in each of the elastic layers with their lines of action in the mid-planes of the elastic layers, such that

$$F_1 = E_1A_1\frac{\partial u_1}{\partial x}, \quad F_3 = E_3A_3\frac{\partial u_3}{\partial x} \tag{4}$$

where A_1 and A_3 are the cross section areas of layers 1 and 3, respectively, and E_1 and E_3 are the corresponding Young's moduli. Since the beam is assumed to be free of longitudinal forces, i.e., $F_1+F_3=0$. Eq. (4) yields the following relationship between the longitudinal deflections of the top and bottom layers:

$$E_1A_1\frac{\partial u_1}{\partial x} = -E_3A_3\frac{\partial u_3}{\partial x} \tag{5}$$

Integration of the above relation with respect to x yields following relation between the longitudinal displacements at the top and bottom layers:

$$u_3 = -eu_1 \tag{6}$$

where $e = E_1A_1/E_3A_3$.

Buna-N rubber is considered as a sealant material around the edges of the MR-fluid layer segment to contain the MR fluid within the two elastic layers of the sandwich beam and maintain uniform thickness. The rubber seal and the MR fluid, however, are modeled as a homogeneous material layer with equivalent shear modulus expressed as

$$\overline{G} = G_r\left(\frac{b_r}{b}\right) + G^*\left(1-\frac{b_r}{b}\right) \tag{7}$$

where $\overline{G}$ is the equivalent shear modulus of the homogeneous layer, b_r and b are the widths of the rubber and the entire beam, respectively, and G_r and G^* are the shear modulus of the rubber and MR fluid, respectively.

The shear stress–shear strain properties of MR fluids have been described in many studies [30,31] and characterized by two distinguished regions, referred to as 'pre-yield' and 'post-yield' regions, as shown in Fig. 2. MR materials experience different levels of stress and strain in response to the applied magnetic field and follow a similar pattern in its rheological behavior. In the pre-yield regime, the MR material demonstrates viscoelastic behavior and is described by the complex modulus as [30]

$$G^*(B) = G'(B) + iG''(B) \tag{8}$$

While the storage modulus $G'(B)$ is proportional to the average energy stored during a cycle of deformation per unit volume of the material, the loss modulus $G''(B)$ is proportional to the energy dissipated per unit volume of the material over a cycle. Moreover, both the moduli are functions of the magnetic field intensity B. The post-yield behavior of MR materials is approximately characterized by the Bingham plastic model, such that [31]

$$\tau = \tau_y + \eta\dot{\gamma} \tag{9}$$

where τ is the shear stress, τ_y is the magnetic field induced dynamic yield stress, η is the plastic viscosity and $\dot{\gamma}$ is the shear strain rate. Due to the application of the magnetic field through MR fluid, the ferrous particle suspended in the viscous fluid produces particle chain and yield stress is thus developed [32]. As a result, both storage and loss moduli (Eq. (8)) increase with increasing magnetic field. Consequently the stiffness and damping properties can be controlled using the applied magnetic field. This enables an effective mechanism to suppress the vibration of the structural systems [21].

2.1. Formulation of energy equations

Lagrange's energy approach has been implemented to formulate the governing equations of motion for the partially treated MR sandwich beam in the finite element form. To accomplish this, the total strain and kinetic energy of the system are derived. The strain energy due to elastic layers located at top and bottom of the sandwich beam, $V_{1,3}$ can be

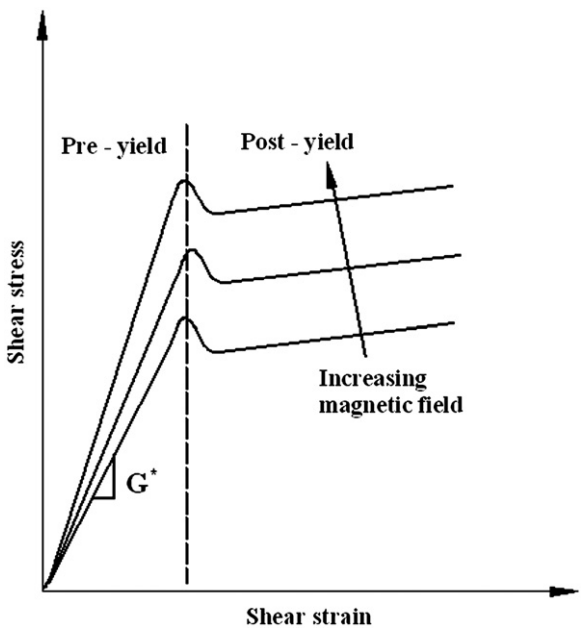

Fig. 2. Shear stress–shear strain relationship of MR materials under varying intensities of magnetic field [29].

expressed as

$$V_{1,3}=\frac{1}{2}\int_0^L (E_1A_1+E_3A_3e^2)\left(\frac{\partial u}{\partial x}\right)^2 \mathrm{d}x+\frac{1}{2}\int_0^L (E_1I_1+E_3I_3)\left(\frac{\partial^2 w}{\partial x^2}\right)^2 \mathrm{d}x \tag{10}$$

where I_1 and I_3 are the second moment of inertia at the centroid of the top and bottom elastic layers 1 and 3, respectively.

The middle layer of the beam consists of elastic and MR fluid segments together with the rubber sealant material and thus the total strain energy of the middle layer of the beam can be expressed as the sum of the strain energy of the MR fluid layer with rubber material, V_{2f} and that of elastic sections, V_{2e}, such that

$$V_2=V_{2f}+V_{2e} \tag{11}$$

The above strain energies for a beam structure with one MR-fluid segment shown in Fig. 1(b), the strain energy associated with each segment can be expressed as

$$V_{2f}=\frac{1}{2}\int_{L_1}^{L_1+L_2} \overline{G}bh_2\left[\frac{D}{h_2}\frac{\partial w}{\partial x}-\frac{(1+e)u}{h_2}\right]^2 \mathrm{d}x$$

and

$$V_{2e}=\frac{1}{2}\int_0^{L_1} E_{2e}A_{2e}\left(\frac{\partial u}{\partial x}\right)^2 \mathrm{d}x+\frac{1}{2}\int_0^{L_1} E_{2e}I_{2e}\left(\frac{\partial^2 w}{\partial x^2}\right)^2 \mathrm{d}x+\frac{1}{2}\int_{L_1+L_2}^{L} E_{2e}A_{2e}\left(\frac{\partial u}{\partial x}\right)^2 \mathrm{d}x+\frac{1}{2}\int_{L_1+L_2}^{L} E_{2e}I_{2e}\left(\frac{\partial^2 w}{\partial x^2}\right)^2 \mathrm{d}x$$

where E_{2e}, A_{2e} and I_{2e} are Young's modulus, cross section area and second moment of inertia, respectively, of the elastic segments within the mid layer of the sandwich beam.

The total strain energy V of the sandwich beam structure is expressed as the sum of those due to top, bottom and middle layers, such that

$$V=V_1+V_2+V_3 \tag{12}$$

The kinetic energy of the sandwich beam structure is derived considering: (i) the transverse motion of the top and bottom elastic layers (T_{1TBL}); (ii) the transverse motion of the middle layer which comprises elastic layer, MR fluid layer and rubber material (T_{1ML}); (iii) the axial deformations of the top and bottom elastic layers (T_2) and (iv) the rotational deformation of the MR fluid segment due to strain displacement (T_3).

The kinetic energy associated with the transverse motions of the top and bottom elastic layers, $T_{1\mathrm{TBL}}$ can be expressed as

$$T_{1\mathrm{TBL}}=\frac{1}{2}\int_0^L (\rho_1A_1+\rho_3A_3)\left(\frac{\partial w}{\partial t}\right)^2 \mathrm{d}x \tag{13}$$

where ρ_1 and ρ_3 are mass densities of the top and bottom elastic layers, respectively.

The kinetic energy associated with the transverse motions of the middle layer of the sandwich beam, $T_{1\mathrm{ML}}$, which comprises elastic and MR fluid layer segments, and rubber material, can be expressed as the sum of the kinetic energy due to transverse motion of the elastic layer, T_{1f}, and that of due to MR fluid layer and rubber material, T_{1e}, such that

$$T_{1\mathrm{ML}}=T_{1f}+T_{1e} \tag{14}$$

where

$$T_{1f}=\frac{1}{2}\int_{L_1}^{L_1+L_2} (\rho_2A_2+\rho_rA_r)\left(\frac{\partial w}{\partial t}\right)^2 \mathrm{d}x$$

$$T_{1e}=\frac{1}{2}\int_0^{L_1} \rho_{2e}A_{2e}\left(\frac{\partial w}{\partial t}\right)^2 \mathrm{d}x+\frac{1}{2}\int_{L_1+L_2}^{L} \rho_2A_{2e}\left(\frac{\partial w}{\partial t}\right)^2 \mathrm{d}x$$

where ρ_2, ρ_{2e} and ρ_r are the mass densities of the MR fluid, elastic layer and the rubber materials, respectively.

The kinetic energy associated with axial deformation of the top and bottom elastic layers, T_2, can be expressed as

$$T_2=\frac{1}{2}\int_0^L (\rho_1A_1+e^2\rho_3A_3)\left(\frac{\partial u}{\partial t}\right)^2 \mathrm{d}x \tag{15}$$

and the kinetic energy associated with the rotation due to shear strain of the MR-fluid layer, T_3, is expressed by

$$T_3=\frac{1}{2}\int_{L_1}^{L_1+L_2} I_2\rho_2\left[\frac{-(1+e)}{h_2}\frac{\partial u}{\partial t}+\frac{D}{h_2}\frac{\partial^2 w}{\partial x\,\partial t}\right]^2 \mathrm{d}x \tag{16}$$

where I_2 is the second moment of inertia at the centroid of the MR-fluid layer.

The total kinetic energy T of the sandwich beam is then obtained from

$$T=T_1+T_2+T_3 \tag{17}$$

It should be noted that apart from the strain and kinetic energies, the work done by the excitation force, if present, also needs to be considered in the formulation. The above equations are also applicable for MR-fluid sandwich beam with either a full-length MR fluid layer or multiple partial MR-fluid segments within the mid-layer.

2.2. Finite element formulation

In finite element analysis (FEM), a standard beam element with two end nodes with three degrees-of-freedom (DOF) for each node is considered. The DOF include the transverse w, axial u and the rotational θ displacements of the beam. The transverse and axial displacements can be expressed in terms of nodal displacement vectors and shape functions, as follows:

$$\mathbf{u}(\mathbf{x},\mathbf{t}) = \mathbf{N_u}(\mathbf{x})\,\mathbf{d}(\mathbf{t}) \tag{18}$$

$$\mathbf{w}(\mathbf{x},\mathbf{t}) = \mathbf{N_w}(\mathbf{x})\,\mathbf{d}(\mathbf{t}) \tag{19}$$

where $\mathbf{d}(\mathbf{t})=\{u^1, w^1, \theta^1, u^2, w^2, \theta^2\}$ and $\mathbf{N_u}(\mathbf{x})$ and $\mathbf{N_w}(\mathbf{x})$ are common linear and cubic polynomial beam shape functions represented as [33]

$$N_1(x) = 1-\frac{x}{l_e}, \quad N_2(x) = 1-\frac{3x^2}{l_e^2}+\frac{2x^3}{l_e^3}, \quad N_3(x) = x-\frac{2x^2}{l_e}+\frac{x^3}{l_e^2}$$

$$N_4(x) = \frac{x}{l_e}, \quad N_5(x) = \frac{3x^2}{l_e^2}-\frac{2x^3}{l_e^3}, \quad N_6(x) = -\frac{x^2}{l_e}+\frac{x^3}{l_e^2} \tag{20}$$

where l_e is the length of the element.

Upon substituting Eqs. (18) and (19) into Eqs. (12) and (17), and subsequently into Lagrange's equations, described as

$$\frac{\mathrm{d}}{\mathrm{d}t}\left(\frac{\partial T}{\partial \dot{q}_i}\right)-\frac{\partial T}{\partial q_i}+\frac{\partial V}{\partial q_i} = Q_i, \quad i = 1,2,3,n \tag{21}$$

the governing equations of motion for the undamped partially or fully treated MR sandwich beam element in the finite element form can be obtained as

$$\mathbf{m^e}\ddot{\mathbf{d}}+\mathbf{k^e}\mathbf{d} = \mathbf{f^e} \tag{22}$$

where n is the total DOF considered in the formulation and Q_i is the generalized force corresponding to the ith DOF, $\mathbf{m^e}$ and $\mathbf{k^e}$ are the element mass and stiffness matrices, respectively, and $\mathbf{f^e}$ is the element force vector. The stiffness and mass matrices of the sandwich beam element containing the MR fluid within its mid-length are summarized in Appendix A. The element matrices of the sandwich beam containing the elastic material within its mid-layer are not presented since the standard matrices are available for such elements. Assembling the mass and the stiffness matrices and the force vector for all the elements, yields the global governing equations of motion of MR sandwich beam which can be expressed in the finite element form as

$$\mathbf{M}\ddot{\mathbf{d}}+\mathbf{K}\mathbf{d} = \mathbf{F} \tag{23}$$

where $\mathbf{M}$, $\mathbf{K}$ and $\mathbf{F}$ are the global system mass and stiffness matrices and global force vector, respectively.

For the partially treated sandwich beam, the matrices $\mathbf{M}$ and $\mathbf{K}$ are formulated by imposing compatibility conditions which are identical transverse and axial displacements and the slopes at the interfaces of the elastic material and MR-fluid segments within the mid-layer of the beam. For the beam with three mid-layer segments, shown in Fig. 1(b), these conditions can be expressed as

$$w_{n-1}(x=L_1) = w_n(x=L_1), \quad w_n(x=L_1+L_2) = w_{n+1}(x=L_1+L_2)$$

$$u_{n-1}(x=L_1) = u_n(x=L_1), \quad u_n(x=L_1+L_2) = u_{n+1}(x=L_1+L_2)$$

$$\theta_{n-1}(x=L_1) = \theta_n(x=L_1), \quad \theta_n(x=L_1+L_2) = \theta_{n+1}(x=L_1+L_2) \tag{24}$$

where w_n, u_n and θ_n refer to the transverse and axial displacements and slope, respectively, of the segment n.

2.3. Ritz formulation

The governing equations of motion of the partially treated MR sandwich beam are also formulated using the Ritz method to analytically obtain the free vibration properties of the partially treated MR sandwich beam, and to examine the validity of the proposed finite-element formulation. For the free vibration problem, the total potential of the system, $\Pi = T+V$, is used to seek a solution of the form:

$$w(x) = \sum_{i=1}^{N} c_i\phi_i \quad \text{and} \quad u(x) = \sum_{j=1}^{N} c_j\phi_j \tag{25}$$

where c_i and c_j are coefficients to be determined, and ϕ_i and ϕ_j are the interpolation functions satisfying the boundary conditions. Substituting Eq. (25) into the potential function, Π, a minimization problem relative to the undetermined coefficients can be established. The application of the stationary condition $\partial\Pi/\partial c_i = 0$, yields a set of N linear simultaneous equations in coefficients $c_1, c_2, \ldots, c_n$ such that

$$[\mathbf{K_R} - \omega^2 \mathbf{M_R}]\mathbf{c} = \mathbf{0} \tag{26}$$

The solution of the above equation yields the natural frequencies and mode shapes of the partially treated MR sandwich beam.

As it can be realized from Eq. (8), both the storage modulus G' and loss modulus G'' are directly dependent on the applied magnetic field B. Thus by changing the magnetic field the stiffness and damping of the MR sandwich beam can be controlled and vibration attenuation can be achieved. The detailed effect of magnetic field on the stiffness matrix can also be realized from the developed element stiffness matrices provided in Appendix A.

3. Experimental study and validation of the developed finite element formulation

Laboratory experiments were performed on a partially treated MR sandwich beam to investigate its essential properties and to examine the validity of the proposed finite element model and Ritz formulation. Two thin aluminum strips (300 mm × 30 mm × 0.9 mm) with zero magnetic permeability were used to fabricate a partially treated MR sandwich beam. The strips were arranged to create a uniform 1.15 mm gap for the MR fluid (MRF-122EG), which was filled only at the center of the mid-layer of the beam over a length of 100 mm and aluminum was located at the remaining portion of the mid-layer, as shown in Fig. 3. In order to maintain the uniform gap and contain the fluid in between the top and bottom layers, 1.15 mm thick high strength Buna-N rubber was applied around the edges using an adhesive. The width of this rubber layer was in the order of 1.5 mm. The sandwich beam was clamped to a support that was mounted on an electro-dynamic vibration exciter, while permanent magnets were used to generate the magnetic field over the beam. Different magnetic field intensity was realized by varying the vertical position of the permanent magnets with respect to the beam, which was measured near the beam surfaces using a Gauss meter. The measurements were performed in the absence of permanent magnets (0 G) and four different positions of the magnets leading to field intensities of approximately 75, 175, 400 and 500 G at the beam surfaces.

Both free and forced vibration responses of the partially treated MR sandwich beam were measured. For the measurement of forced response, a single-axis accelerometer, oriented along the z-axis, was installed close to the free edge of the beam, to measure the acceleration response. A single-axis accelerometer was also installed at the support to measure the acceleration due to excitation. This acceleration signal also served as the feedback for the vibration exciter controller. The schematic and photograph of the experimental setup is shown in Fig. 4. The forced vibration responses of the partially treated MR sandwich beam were measured under a white-noise vibration spectrum with nearly constant power spectrum density (PSD) in the 1–300 Hz frequency range at three different magnetic field intensities (0, 75 and 175 G). The forced responses were measured in terms of the transfer function of the accelerations at the free end and the support, using the H_1 function of the signal analyzer (Bruel & Kjaer 2035). The natural frequencies of the sandwich beam were subsequently identified from the peaks in the frequency response function. The forced vibration response could not be performed under higher magnetic field intensities (400 and 500 G) due to very small clearance between the beam and magnets, which caused repetitive locking of the beam with the magnets. The natural frequencies under these fields were thus extracted from the frequency spectrum of the free vibration response of the partially treated MR sandwich beam to a very low-level perturbation. The complex shear modulus of the MR fluid, MRF-122EG, used in the test specimen was estimated by performing a free oscillation experiment on the fully treated MR sandwich beam [26]. Both the storage and shear moduli were expressed by the following second-order polynomial function with respect to the magnetic field intensity:

$$G'(B) = -3.3691B^2 + 4997.5B + 0.873 \times 10^6$$

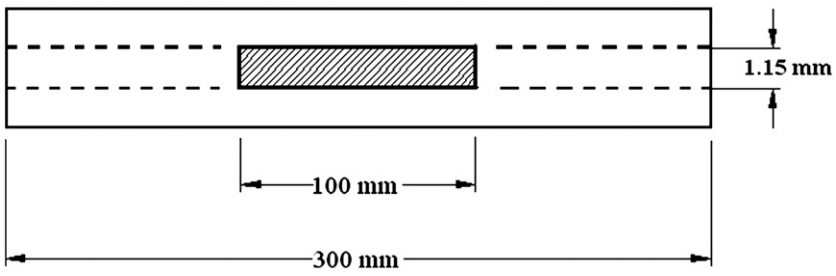

Fig. 3. The test specimen of a partially treated MR fluid sandwich beam.

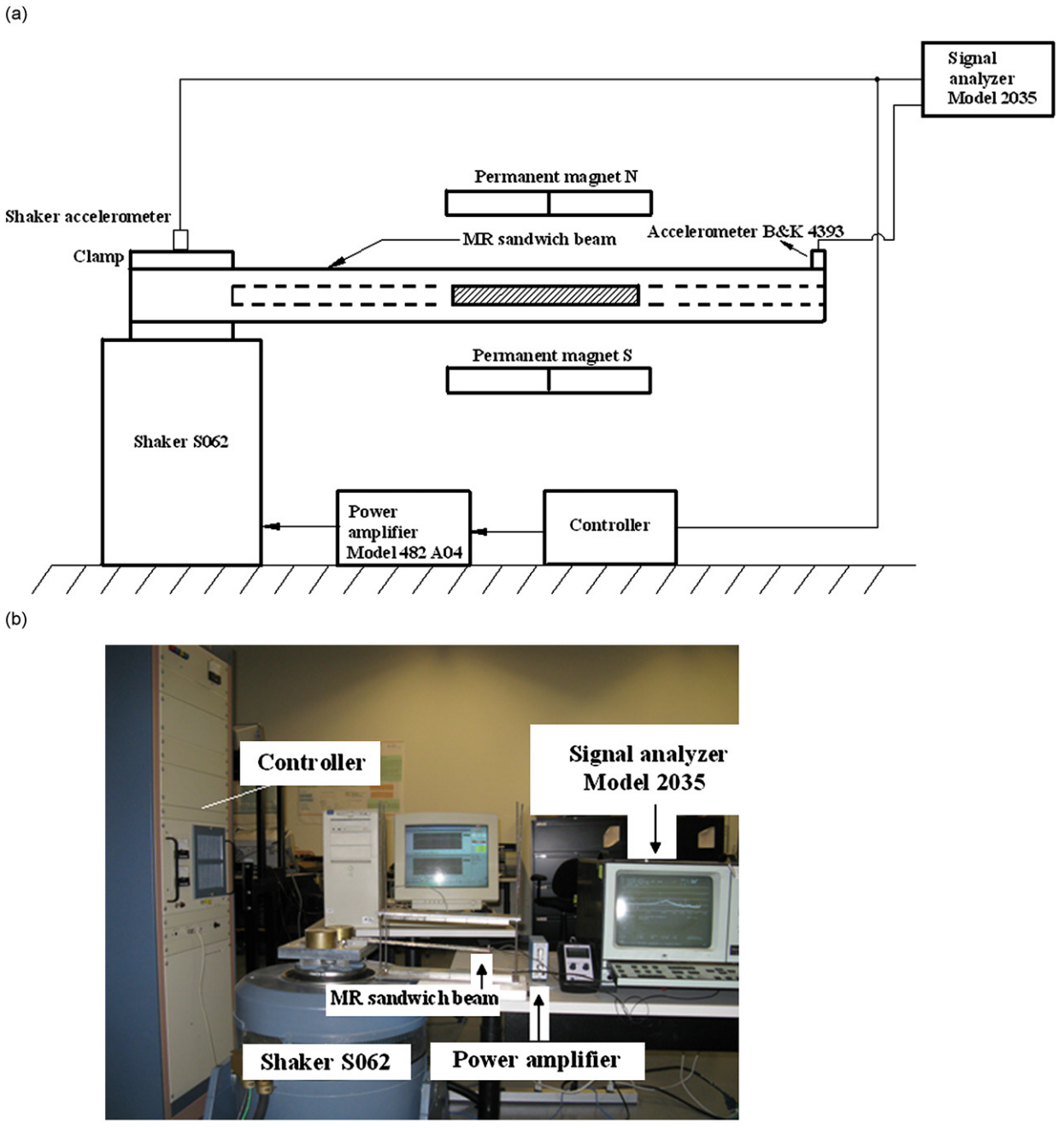

Fig. 4. Experimental setup: (a) block diagram of the experimental setup, and (b) photograph of the partially treated MR sandwich beam experimental setup.

$$G''(B) = -0.9B^2 + 0.8124 \times 10^3 B + 0.1855 \times 10^6 \tag{27}$$

Now the developed finite element and Ritz formulations for the partially treated MR sandwich beam are validated by comparing the computed natural frequencies with those identified from the free and forced vibration responses of the beam. The simulations were performed by considering the material properties as: $\rho_1=\rho_3=2700\,\text{kg/m}^3$; $E_1=E_3=68\,\text{GPa}$; $\rho_r=1233\,\text{kg/m}^3$ and $\rho_2=3500\,\text{kg/m}^3$. Table 1 lists the comparisons of the natural frequencies obtained from the FEM and Ritz formulations with those obtained experimentally for the first three modes under different field intensities. A good agreement could be observed between the computed and measured frequencies, irrespective of the field intensity and the mode. Furthermore, the results obtained from the proposed finite element model are in close agreement with those derived from the Ritz method for the range of field intensities and modes considered.

Table 1
Comparison of natural frequencies of a partially treated cantilever MR-sandwich beam derived from the finite-element and Ritz formulations with the measured frequencies.

Field intensity (G)	Mode	Natural frequencies (Hz)				
		Measured	FEM		Ritz method	
			Results	Percent deviation	Results	Percent deviation
0	1	15	15.88	5.54	14.79	1.40
	2	85	80.96	4.75	83.13	2.20
	3	228	222.55	2.39	220.61	3.24
75	1	16	17.06	6.21	16.26	1.60
	2	87	82.26	5.45	85.88	1.29
	3	231	225.46	2.39	224.34	2.88
175	1	17	18.16	6.39	17.72	4.06
	2	90	83.68	7.02	88.52	1.64
	3	235	228.54	2.75	228.50	2.77
400	1	19	19.56	2.86	19.71	3.60
	2	94	85.81	8.71	93.19	0.86
	3	239	233.08	2.48	234.94	1.70
500	1	21	19.89	5.29	20.20	3.81
	2	95	86.37	9.08	94.33	0.71
	3	240	234.26	2.39	236.68	1.38

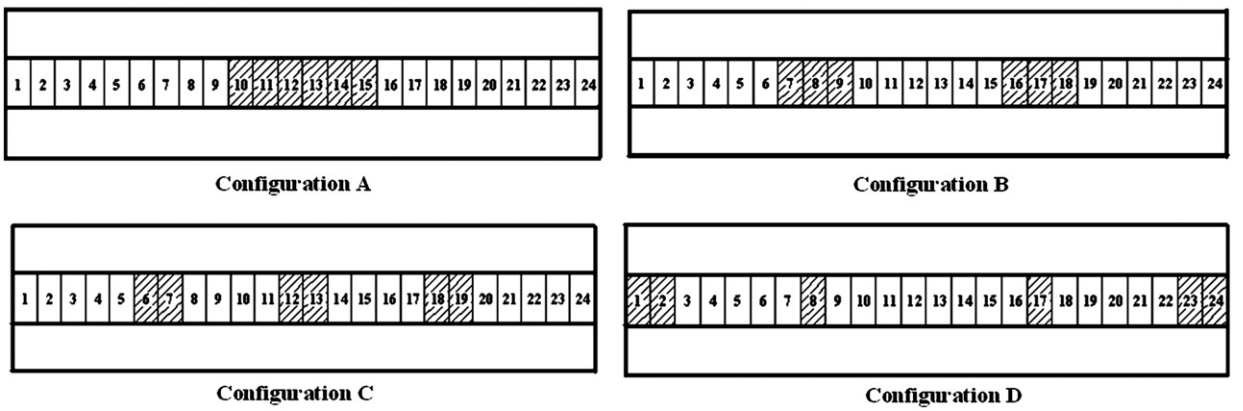

Fig. 5. Various configurations of partially treated MR fluid sandwich beam.

4. Parametric studies

The properties of a partially treated MR-fluid sandwich beam are strongly influenced by many fluid and structure-related parameters such as field intensity, fluid layer thickness, complex shear modulus of the MR fluid, beam geometry and boundary conditions. Apart from these, the properties could also be identified by the number, size and locations of the MR-fluid segments in case of a partially treated structure. Here in this study, the proposed finite element model is used to investigate the effects of variations in the location and lengths of the MR fluid segment of the beam on the natural frequencies and loss factor under different magnetic field intensities. The influence of length and locations of such segments on the transverse vibration response are also investigated. For this purpose four different configurations of the localized MR damping treatments, denoted as 'A', 'B', 'C' and 'D' (Fig. 5), are considered together with different boundary conditions namely simply supported (SSB), clamped–free (CFB) and clamped–clamped (CCB). The total length of the multi-layer beam is divided into 24 segments of equal length, while the MR fluid treatment is applied to selected segments or pockets of the structure. The remaining segments of the beam are considered to be of aluminum material. The total length of the MR fluid layer in all the configurations is assumed to be constant to facilitate relative property analyses. The simulation results are obtained by considering identical baseline thickness of 1 mm of the elastic and fluid layers, while the material and all other properties of the layers are identical to those described in Section 3.

The validity of the developed finite element formulations for the four different configurations considered has been demonstrated by comparing the natural frequencies corresponding to the first three modes obtained through FEM with

Ritz formulation under simply supported end conditions without any magnetic field and the results are presented in Table 2. A good agreement could be observed between the natural frequencies computed through FEM and Ritz formulations.

4.1. Influence of magnetic field intensity on natural frequencies

The influence of variations in the magnetic field intensity on the natural frequencies for the different configurations of a partially treated MR sandwich beam is investigated under different end conditions. The results attained from the FEM in terms of natural frequencies corresponding to the first five modes are summarized in Tables 3 and 4 for the four configurations subject to three different field intensities (0, 250 and 500 G). It can be seen from Table 3 that the natural frequencies corresponding to all the modes increase with increasing magnetic field, irrespective of the configuration considered. The increase in the natural frequencies with increasing magnetic field can be attributed to increase in the complex shear modulus of the MR fluid and thus the structure stiffness under a higher magnetic field, which is evident from the element stiffness matrix presented in Appendix A. This confirms the potential of the MR fluid treatment to control the response of the structure. This trend of increasing natural frequency with the applied magnetic field intensity has also been represented in fewer studies on fully treated beams [21–24,26].

Table 4 summarizes the influence of variations in different boundary conditions, including the simply supported (SSB), clamped–free (CFB) and clamped–clamped (CCB) conditions, on the natural frequencies of a partially treated MR-fluid sandwich beam structure at a magnetic field intensity of 500 G. The results are presented for all the four configurations and

Table 2
Comparison of natural frequencies of a partially treated simply supported MR-sandwich beam derived from the finite-element with Ritz formulations at the magnetic field of 0 G.

Configuration	Mode	Natural frequencies (Hz)		
		FEM	Ritz method	Percent deviation
A	1	28.30	29.04	2.55
	2	198.14	201.65	1.74
	3	473.74	475.71	0.41
B	1	33.40	33.93	1.56
	2	113.58	114.95	1.19
	3	484.07	486.35	0.47
C	1	34.16	35.29	3.20
	2	126.21	125.29	0.73
	3	270.68	269.75	0.34
D	1	50.10	49.94	0.32
	2	163.94	164.70	0.46
	3	473.99	476.58	0.54

Table 3
Influence of variations in the magnetic field intensity on the natural frequencies of different configurations of a partially treated simply supported MR sandwich beam.

Field intensity (G)	Configuration	Mode number				
		1	2	3	4	5
0	A	28.30	198.14	473.74	694.21	1114.10
	B	33.40	113.58	484.07	742.85	1247.70
	C	34.16	126.21	270.68	906.34	1170.50
	D	50.10	163.94	473.99	605.89	965.40
250	A	29.86	206.33	479.52	700.13	1127.60
	B	35.61	116.02	493.07	751.09	1252.10
	C	36.63	129.05	273.94	915.50	1177.80
	D	54.20	168.26	484.31	616.8	970.44
500	A	30.68	210.47	482.73	703.46	1135.30
	B	36.77	117.38	498.14	755.59	1254.60
	C	37.95	130.62	275.82	920.79	1182.00
	D	56.37	170.64	490.24	623.16	973.41

Table 4
Influence of variations in the end conditions on the natural frequencies of the fully and partially treated MR sandwich beams at the magnetic field of 500 G.

End conditions	Configuration		Mode number				
			1	2	3	4	5
Simply supported	Fully treated beam		55.89	128.95	233.97	371.00	543.05
	Partially treated beam	A	30.68	210.47	482.73	703.46	1135.30
		B	36.77	117.38	498.14	755.59	1254.60
		C	37.95	130.62	275.82	920.79	1182.00
		D	56.37	170.64	490.24	623.16	973.41
Clamped–free	Fully treated beam		16.23	82.20	180.78	302.78	458.30
	Partially treated beam	A	20.36	88.31	285.59	655.09	934.52
		B	18.31	101.18	212.42	608.96	911.77
		C	18.07	97.42	239.26	383.43	1061.80
		D	13.27	94.73	227.70	690.62	988.36
Clamped–clamped	Fully treated beam		70.75	162.30	285.50	440.48	629.52
	Partially treated beam	A	113.69	300.24	654.74	931.05	1320.60
		B	139.03	241.52	628.35	924.01	1525.00
		C	117.61	299.61	411.70	1076.80	1450.00
		D	74.87	201.83	649.90	903.64	1168.30

compared with those of fully treated MR sandwich beams subject to the same magnetic field. It can be observed that the natural frequencies of the partially treated beam are generally greater than those of the fully treated beam, irrespective of the configuration, end conditions and modes of vibration. This is primarily attributed to the contributions of the aluminum segment replacing the MR fluid in the partially treated configurations, which also yields lower mass compared to the fully treated beam. The above trend, however, is not evident for the fundamental and second mode of the configurations A, B & D and B, respectively, with simply supported end conditions and fundamental mode of the configuration D with clamped–free end conditions, which can be related to the relative changes in the stiffness and mass corresponding to the fundamental mode. In other words, even though the mass of the beam has been decreased considerably in partially treated configurations compared to the fully treated beam, the decrease in stiffness would be relatively larger than that of mass corresponding to the fundamental mode. The results also show that depending on the mode of vibration, the natural frequency of a particular partially treated configuration may be considerably higher than those of the other configuration, irrespective of the end conditions, which can also be related to the relative changes in the stiffness and mass of the beam. Furthermore, as expected, the clamped–clamped and clamped–free end conditions yield the highest and the lowest natural frequencies, respectively, for all modes considered, irrespective of the magnetic field intensity and the treatment configuration considered.

4.2. *Influence of magnetic field intensity on loss factor*

The loss factor is computed as the ratio of the square of the imaginary component of the complex natural frequency to that of the real component [21]. The influence of variations in the magnetic field intensity on the loss factor corresponding to the first five modes for the various configurations of a partially treated MR sandwich beam is investigated and compared with those of fully treated MR sandwich beam for different end conditions under magnetic field intensities of 0, 250 and 500 G and the results are summarized in Table 5. The results generally show that the loss factor increases with increasing magnetic field intensity for all the configurations considered. The loss factor is merely the ratio of energy dissipated per radian to the total strain energy, both of which increase with the magnetic field. Furthermore, the dissipated energy is directly related to the loss modulus, which increases with the field intensity as seen in Eq. (27). The relative increase in the loss modulus and thus the dissipated energy with increase in the magnetic field, however, is greater than that in the total strain energy, which leads to higher loss moduli under increasing magnetic field. This trend of increasing loss factor with the applied magnetic field intensity has also been represented in fewer studies on fully treated beams [21–24,26].

The above trend, however, is not evident for the fundamental mode under simply supported and clamped–free end conditions and few higher modes such as mode 3, mode 5 and modes 2 and 3 for the configurations A, B and D, respectively, under clamped–free end conditions. It increases considerably under the application of the magnetic field of intensity up to 250 G but decreases slightly with further increase in the field intensity. This can be attributed to the relative changes in the dissipated and strain energy corresponding to the fundamental mode. The increase in the total strain energy related to the corresponding mode with the magnetic field would be relatively smaller compared to that of energy dissipated resulting in increase in the loss factor until the magnetic field reaches a certain value. However, a further increase in magnetic field yields higher relative change in the total strain energy at the corresponding mode compared to that of the energy dissipated, which results in slightly lower loss factor.

Table 5
Influence of variations in the magnetic field intensity on the loss factor for the various configurations of a partially treated MR sandwich beam under different end conditions.

End condition	Field intensity (G)	Configuration		Mode number				
				1	2	3	4	5
SSB	0	Fully treated beam		0.0999	0.0603	0.0384	0.0253	0.0176
		Partially treated beam	A	0.0190	0.0147	0.0041	0.0029	0.0039
			B	0.0230	0.0072	0.0062	0.0038	0.0011
			C	0.0249	0.0076	0.0039	0.0033	0.0021
			D	0.0283	0.0089	0.0072	0.0059	0.0017
	250	Fully treated beam		0.1077	0.0772	0.0559	0.0400	0.0292
		Partially treated beam	A	0.0292	0.0210	0.0070	0.0049	0.0071
			B	0.0346	0.0122	0.0107	0.0063	0.0021
			C	0.0380	0.0127	0.0071	0.0059	0.0036
			D	0.0424	0.0148	0.0126	0.0106	0.0031
	500	Fully treated beam		0.0941	0.0719	0.0545	0.0405	0.0304
		Partially treated beam	A	0.0291	0.0215	0.0073	0.0052	0.0077
			B	0.0342	0.0128	0.0112	0.0065	0.0023
			C	0.0377	0.0132	0.0076	0.0064	0.0039
			D	0.0419	0.0153	0.0135	0.0114	0.0034
CFB	0	Fully treated beam		0.0581	0.0597	0.0483	0.0323	0.0224
		Partially treated beam	A	0.0458	0.0082	0.0096	0.0044	0.0019
			B	0.0485	0.0137	0.0033	0.0047	0.0034
			C	0.0492	0.0154	0.0044	0.0020	0.0029
			D	0.0436	0.0144	0.0055	0.0030	0.0042
	250	Fully treated beam		0.0518	0.0661	0.0615	0.0472	0.0353
		Partially treated beam	A	0.0485	0.0133	0.0136	0.0076	0.0034
			B	0.0520	0.0214	0.0059	0.0080	0.0051
			C	0.0530	0.0240	0.0078	0.0036	0.0053
			D	0.0493	0.0197	0.0081	0.0049	0.0066
	500	Fully treated beam		0.0431	0.0588	0.0570	0.0462	0.0357
		Partially treated beam	A	0.0414	0.0137	0.0132	0.0080	0.0036
			B	0.0447	0.0216	0.0063	0.0085	0.0050
			C	0.0456	0.0242	0.0084	0.0039	0.0057
			D	0.0439	0.0189	0.0081	0.0051	0.0067
CCB	0	Fully treated beam		0.0566	0.0381	0.0262	0.0183	0.0133
		Partially treated beam	A	0.0039	0.0106	0.0045	0.0020	0.0029
			B	0.0059	0.0024	0.0045	0.0038	0.0013
			C	0.0076	0.0028	0.0016	0.0029	0.0021
			D	0.0079	0.0027	0.0022	0.0022	0.0013
	250	Fully treated beam		0.0702	0.0536	0.0405	0.0301	0.0227
		Partially treated beam	A	0.0066	0.0162	0.0077	0.0035	0.0054
			B	0.0098	0.0043	0.0079	0.0063	0.0024
			C	0.0130	0.0049	0.0030	0.0052	0.0037
			D	0.0137	0.0049	0.0040	0.0041	0.0023
	500	Fully treated beam		0.0640	0.0515	0.0406	0.0310	0.0239
		Partially treated beam	A	0.0069	0.0161	0.0081	0.0038	0.0059
			B	0.0101	0.0046	0.0084	0.0065	0.0026
			C	0.0136	0.0053	0.0033	0.0056	0.0040
			D	0.0145	0.0053	0.0043	0.0044	0.0025

It can also be observed that all the configurations with clamped–free and clamped–clamped end conditions yield the highest and lowest loss factors, respectively, among the end conditions considered at all levels of magnetic field. This can be related to the fact that the clamped–clamped and clamped–free end conditions have the highest and lowest strain energies, respectively, which result the corresponding lowest and highest loss factors.

Furthermore, the results show that the loss factor due to the fully treated MR sandwich beam is generally higher than those of the partially treated beams irrespective to the configurations and end conditions considered. This can be attributed to the relatively smaller length of the MR fluid layer in partially treated beams compared to that of the fully treated beam, which yields lower dissipated energy. The above trend, however, is not evident for the fundamental mode of the configurations B and C at magnetic field intensity of 250 G and B, C and D with magnetic field intensity of 500 G under clamped–free end conditions. This can be again related to the relative changes in the dissipated energy and the total strain energy at the lower mode. The increase in the strain energy of the partially treated beam corresponding to the lower modes would be relatively smaller than that of the dissipated energy.

4.3. Influences of location of MR fluid

The results presented in Tables 3–5 clearly illustrate the influence of location of the MR-fluid segments on both the natural frequencies and loss factors corresponds to the first five modes in which the total length of the MR fluid treatment is identical in all the configurations. The influence of location of the treatment is further investigated by considering the configuration A with simply supported and clamped–free end conditions. Four different locations of the partial treatment are considered for the analysis, as shown in Fig. 6. The 75 mm MR fluid treatment is applied over six different consecutive elements of the 24-element sandwich beam, which are denoted as A1, A2, A3 and A4 involving fluid treatments over 1–6, 7–12, 13–18 and 19–24 elements, respectively, as shown in Fig. 6. The results obtained in terms of natural frequencies and loss factor corresponding to the first five modes of the four arrangements are summarized in Tables 6 and 7, respectively, under a magnetic field of 500 G. The tables also illustrate the results attained for configuration A, where the treatment is applied over elements 10–15. It can be observed that due to the nature of the symmetry of the simply supported end conditions, the natural frequencies and the loss factor for A1 & A4 and A2 & A3 arrangements are identical. The above trend, however, is not evident for the asymmetric clamped–free end conditions. It can also be seen that locating the MR-fluid segments at the boundary edges of the simply supported end conditions generally yields the higher loss factor except in the modes 2 and 4. For modes 2 and 4, locating the MR-fluids segments at the mid-span of the beam yields higher loss factor. It should be noted that such type variation could not be observed under clamped–free end conditions. However, the results generally show that the location of MR fluid pockets significantly affect the natural frequency and loss factor, irrespective of the end conditions and the mode of vibration.

The effect of location of the MR-fluid treatment is further investigated by evaluating the deflection modes corresponding to the first four modes. For this purpose, the mode shapes of the four configurations of the partially treated simply supported beam are evaluated. Fig. 7 illustrates the first four mode shapes of the partially treated MR sandwich beam. The results are attained in the absence of the magnetic field and compared with those of a fully treated beam. The results suggest that the partial treatment of the beam could alter the deflection mode, particularly the location of the peak normalized deflection. A fully treated beam, owing to its symmetry consistently reveals harmonic deflection

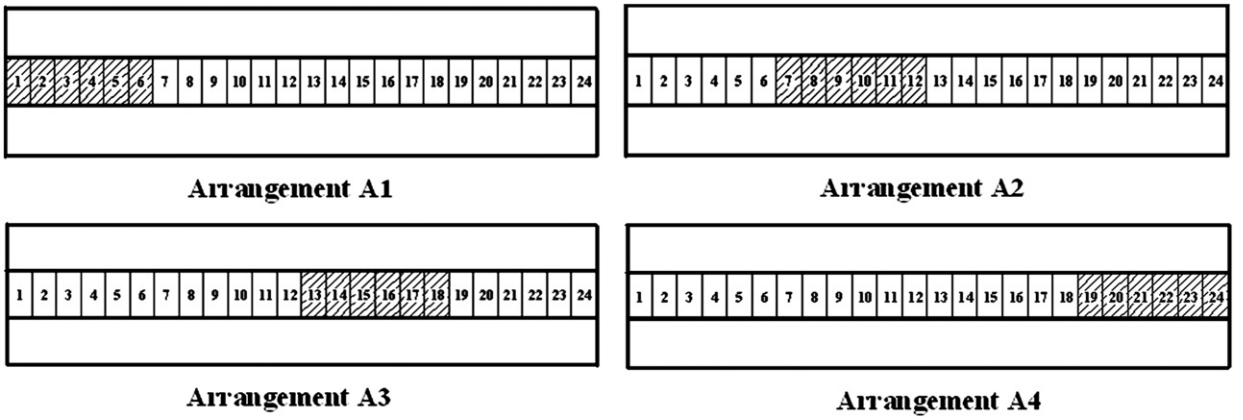

Fig. 6. Different arrangements of configuration A of a partially treated MR sandwich beam.

Table 6
Influence of variations in the location of MR fluid on the natural frequency of configuration A of the partially treated MR sandwich beam at the magnetic field of 500 G.

End conditions	Mode number	Natural frequency (Hz)				
		A (10–15)	A1 (1–6)	A2 (7–12)	A3 (13–18)	A4 (19–24)
Simply supported	1	30.68	68.51	33.62	33.62	68.51
	2	210.47	190.59	203.51	203.51	190.59
	3	482.73	470.71	412.89	412.89	470.71
	4	703.46	740.77	816.49	816.49	740.77
	5	1135.30	1190.90	1205.40	1205.40	1190.90
Clamped–free	1	20.36	10.49	16.38	24.76	28.48
	2	88.31	113.10	106.08	85.31	150.89
	3	285.59	282.45	319.09	278.21	297.29
	4	655.09	617.74	557.30	540.04	628.62
	5	934.52	937.36	980.27	972.65	952.46

Table 7
Influence of variations in the location of MR fluid on the loss factor of configuration A of the partially treated MR sandwich beam at the magnetic field of 500 G.

End conditions	Mode number	Loss factor				
		A (10–15)	A1 (1–6)	A2 (7–12)	A3 (13–18)	A4 (19–24)
Simply supported	1	0.02908	0.05066	0.03343	0.03343	0.05066
	2	0.02145	0.02005	0.01746	0.01746	0.02005
	3	0.00731	0.01081	0.00956	0.00956	0.01081
	4	0.00523	0.01082	0.00888	0.00888	0.01082
	5	0.00766	0.00361	0.00320	0.00320	0.00361
Clamped–free	1	0.04135	0.04952	0.04591	0.03042	0.01182
	2	0.01371	0.02164	0.01448	0.02241	0.01865
	3	0.01319	0.00887	0.00947	0.01303	0.01575
	4	0.00797	0.00567	0.00652	0.00585	0.01020
	5	0.00361	0.00733	0.00858	0.00872	0.01391

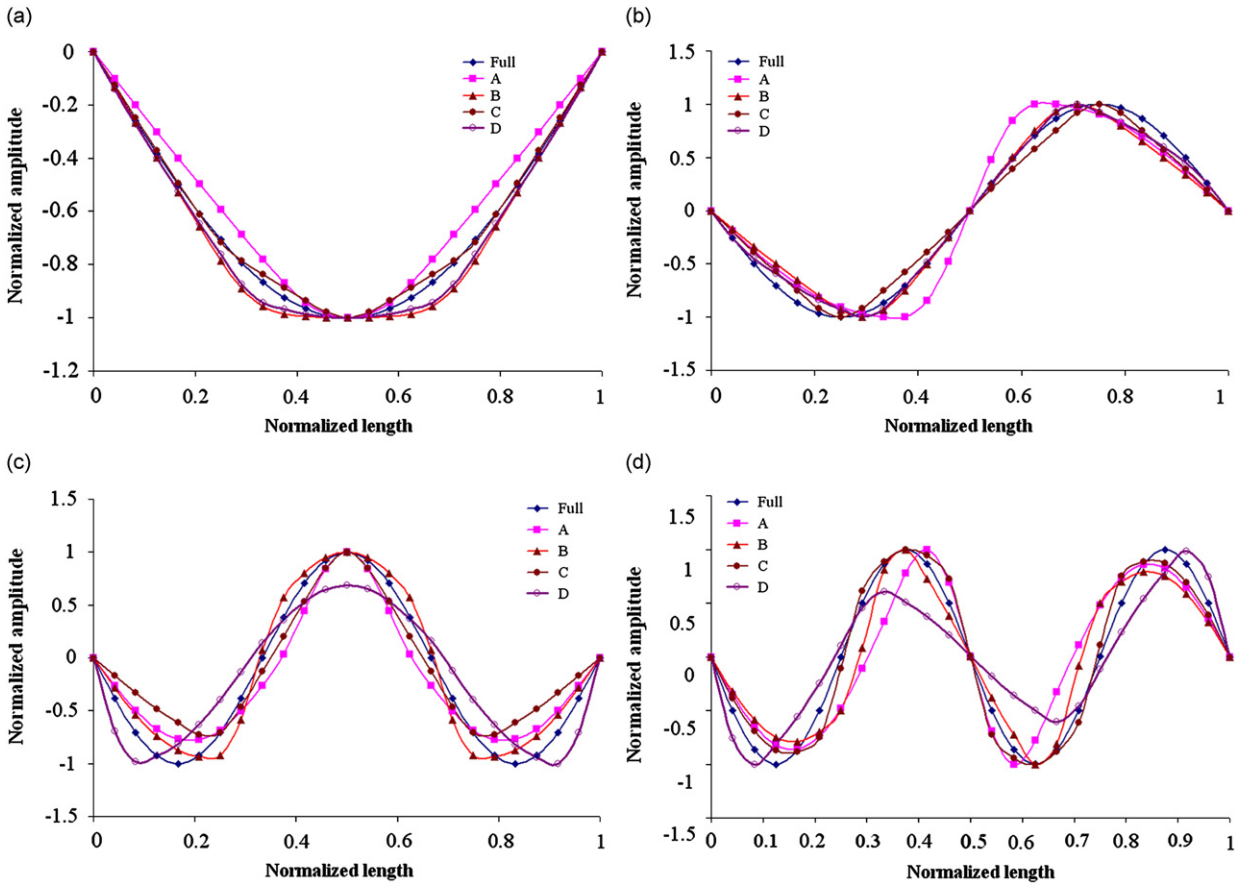

Fig. 7. First four mode shapes of the fully and partially treated MR sandwich beam without applying magnetic field: (a) Mode 1, (b) Mode 2, (c) Mode 3, and (d) Mode 4.

patterns. The above trend could not be observed in partially treated beams due to the partial location of MR-fluid segments. However, it can be observed that the configuration D yields the lowest peak deflection mode shape under modes 3 and 4. This can be attributed to the highest loss factor at the corresponding modes which is evident from Table 5. Although the configuration D yields higher loss factor even at the fundamental mode, such type of variation could not be observed. This can be related to the fact that the total strain energy dominates the dissipated energy as it can be realized from Table 3. This yields the higher natural frequency and hence the configuration D at mode 1 could not yield lower peak deflection mode shape.

4.4. Influence of the length of MR fluid layer

The influences of variation in the length of MR fluid treatment on the natural frequencies of a simply supported partially treated MR beam (configuration A) is further investigated under the magnetic field of 500 G. The simulations are performed by considering MR fluid treatments over 25, 50, 75 and 100 percent of the beam length. Fig. 8 illustrates the variations in the natural frequencies of the configuration A with different lengths of the treatment corresponding to the first five modes. The results show significant effect of the fluid treatment length on the higher mode natural frequencies, while the effect is small on the lower modes. The results generally show a decrease in the higher modes natural frequencies with increasing length of the MR-fluid treatment, although the effect is highly nonlinear. This can be attributed to relatively greater change in the beam mass than that in the stiffness corresponding to higher modes, when the length of MR-fluid layer is increased. This trend, however, is not evident for the fundamental mode frequency, where the relative variation in the beam stiffness could be greater than that in the beam mass with increasing the fluid treatment length.

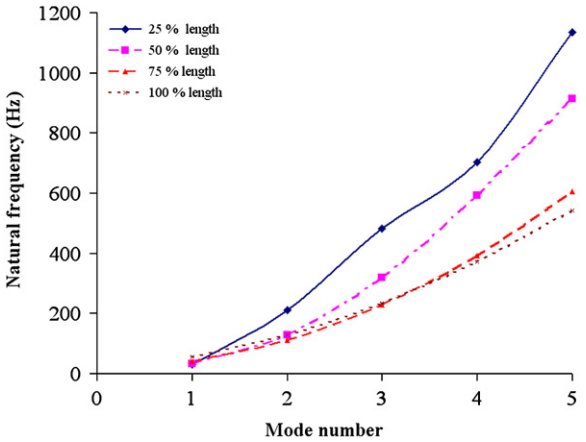

Fig. 8. Influence of MR fluid layer length on the natural frequencies of a simply supported partially treated MR sandwich beam (configuration A) under the magnetic field of 500 G.

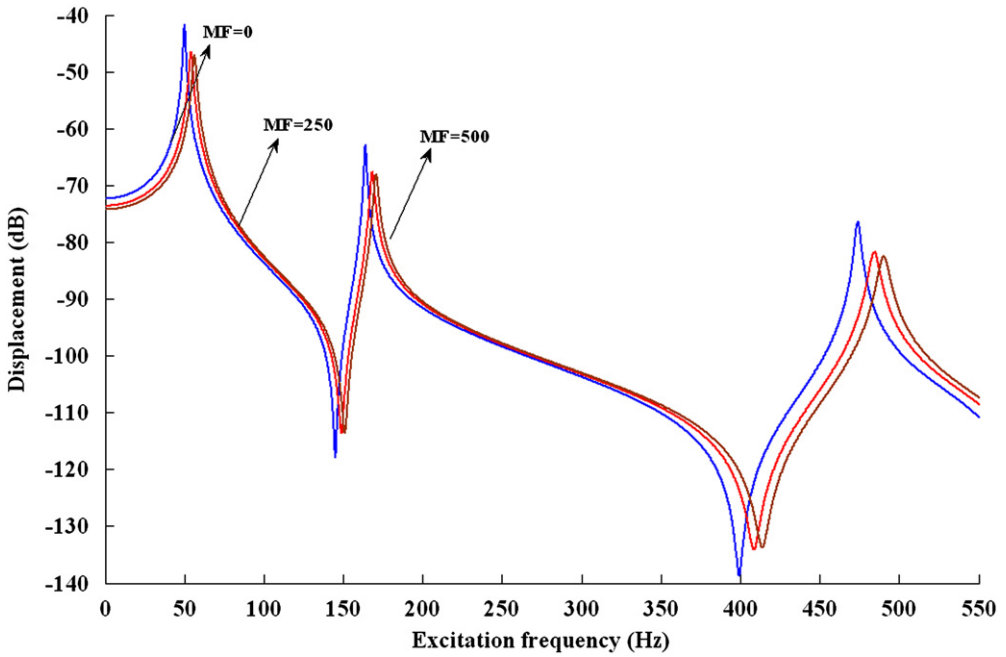

Fig. 9. Influence of magnetic field on the transverse response of configuration D of a simply supported partially treated MR fluid sandwich beam.

4.5. Transverse response of the partially treated MR sandwich beam

The influence of magnetic field on the transverse response of configuration D of a simply supported partially treated MR sandwich beam is investigated by considering sinusoidal excitation applied at a distance of 175 mm from the left support. The dynamic response characteristics of the beam were simulated under a 1 N force excitation over the frequency range of 1–550 Hz for three different magnetic field intensities of 0, 250 and 500 G. The amplitude spectrum of the transverse displacement was evaluated at a distance of 187.5 mm from the left support and is illustrated in Fig. 9. The results show increase in the natural frequencies (frequencies corresponding to response peaks) with increasing magnetic field, as observed from the free vibration responses. The peak response magnitudes corresponding to all the modes also decrease with increasing magnetic field, which may be attributed to higher loss factors under higher magnetic fields. The changes in the peak magnitudes, however, appear to be nonlinear functions of the magnetic field. An increase in the magnetic field from 0 to 250 G yields substantial reduction in the peak amplitudes, which are approximately 11.6, 7.5 and 6.9 percent, respectively, for the first three modes considered in the analysis.

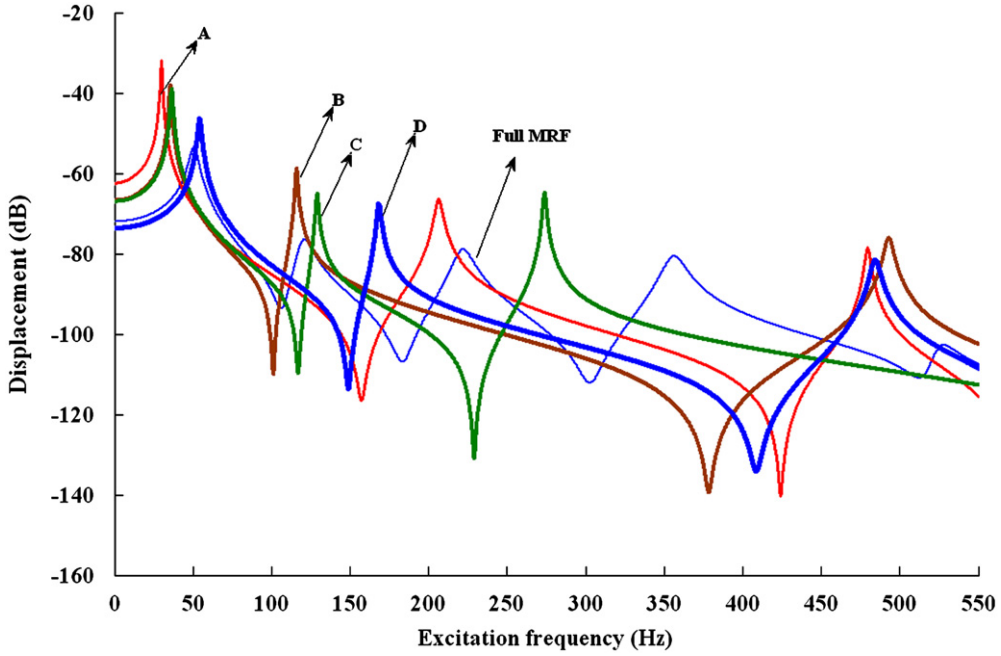

Fig. 10. Transverse displacement of fully and partially treated MR sandwich beam at a magnetic field of 250 G under simply supported end conditions.

Table 8
Location and magnitude of the maximum displacement of transverse displacement at magnetic field of 500 G for simply supported end conditions.

Excitation frequency (Hz)	Configuration	Location of the maximum displacement from the left end (mm)	Magnitude of the maximum displacement (mm)
30.23	Fully treated	181	0.212
	A	168	0.748
	B	207	0.438
	C	168	0.441
	D	194	0.195
38.20	Fully treated	181	0.212
	A	168	0.752
	B	207	0.439
	C	168	0.442
	D	194	0.195
57.29	Fully treated	181	0.213
	A	168	0.767
	B	207	0.445
	C	168	0.448
	D	194	0.196

The transverse response of various configurations of simply supported partially treated MR sandwich beams is also evaluated and compared with that of fully treated MR sandwich beam at a magnetic field of 250 G by considering a sinusoidal excitation force of 1 N magnitude acting at a distance of 175 mm from the left support. Again, the transverse displacement is calculated at a distance of 187.5 mm from the left support over a frequency range of 1–550 Hz and the results are shown in Fig. 10. Furthermore, the magnitude and location (from the left end) of the maximum displacement of the beam under the magnetic field of 500 G are evaluated at various excitation frequencies (30.23, 38.20 and 57.29 Hz) which are approximately equal to the first natural frequency of fully and various configurations of partially treated MR sandwich beam and compared with that of fully treated MR sandwich beam. The results are listed in Table 8. It can be observed that for the same excitation frequency the location of the maximum displacement differs for the various configurations. Also the minimum magnitude of the maximum displacement occurs in the configuration D and is approximately equal to that of fully treated MR sandwich beam for the excitation frequencies considered in the analysis. This can be related to the higher loss factor for the fully treated and configuration D of the partially treated MR sandwich beam which is evident from Table 5. It can also be observed that the largest magnitude of maximum displacement occurs at the configuration A for all the excitation frequencies considered in the analysis. This is due to the fact that the configuration A has the lowest loss factor at the fundamental mode as evident from Table 5. This confirms that the MR fluid could be applied at any critical locations of the structure to suppress the vibration effectively.

5. Conclusions

In this study, vibration response of a partially treated multi-layered beam with MR fluid as a sandwich layer between two layers of the continuous elastic structure has been analyzed. First, mathematical model of the partially treated MR composite beam was developed in finite element form and Ritz formulation to simulate the dynamic response of the system. The experimental study is then conducted to characterize the MR fluid behavior and to validate the developed formulations. Using the developed finite element formulation, different configurations of a partially treated MR sandwich beam has been studied and then various parametric studies have been conducted to demonstrate the controllable capabilities. It has been shown that the location and length of the MR fluid segments have significant effect on the natural frequencies and the loss factor of the partially treated MR sandwich structure in addition to the intensity of the magnetic field and the boundary conditions. It has been demonstrated that the MR fluid pockets should be located at a particular location depending on the boundary conditions and the mode of vibration to be controlled for the effective vibration suppression. Furthermore, the mode shape of the partially treated MR sandwich beam could be controlled by locating the MR fluid layers at the desired locations. It has also been shown that the natural frequency at the higher modes could be increased with decreasing the length of MR fluid layer. Transverse response of a partially treated MR sandwich beam also confirms that the amplitude of vibration could be considerably reduced using controllable MR fluids and conveniently applied them to partial or more critical components of a large structure to realize more efficient vibration control.

Appendix A. Coefficients of element stiffness and mass matrices for the partially treated MR fluid multi-layer beam

The symmetric (6×6) elemental mass and stiffness matrices derived using Lagrange's energy equation are summarized below.

Stiffness matrix of the sandwich beam element comprising MR fluid within the mid-layer:

$$k_{11}=\int_0^{l_e}\alpha_1\dot{N}_1^2\,dx+\int_0^{l_e}\alpha_2N_1^2\,dx,\quad k_{12}=\int_0^{l_e}\alpha_3N_1\dot{N}_2\,dx,\quad k_{13}=\int_0^{l_e}\alpha_3N_1\dot{N}_3\,dx$$

$$k_{14}=\int_0^{l_e}\alpha_1\dot{N}_1\dot{N}_4\,dx+\int_0^{le}\alpha_2N_1N_4\,dx,\quad k_{15}=\int_0^{le}\alpha_3N_1\dot{N}_5\,dx,\quad k_{16}=\int_0^{le}\dot{\alpha}_3N_1\dot{N}_6\,dx$$

$$k_{22}=\int_0^{l_e}\alpha_4\ddot{N}_2^2\,dx+\int_0^{l_e}\alpha_5\dot{N}_2^2\,dx,\quad k_{23}=\int_0^{l_e}\alpha_4\ddot{N}_2\ddot{N}_3\,dx+\int_0^{l_e}\alpha_5\dot{N}_2\dot{N}_3\,dx,\quad k_{24}=\int_0^{l_e}\alpha_3\dot{N}_2N_4\,dx$$

$$k_{25}=\int_0^{l_e}\alpha_4\ddot{N}_2\ddot{N}_5\,dx+\int_0^{l_e}\alpha_5\dot{N}_2\dot{N}_5\,dx,\quad k_{26}=\int_0^{l_e}\alpha_4\ddot{N}_2\ddot{N}_6\,dx+\int_0^{l_e}\alpha_5\dot{N}_2\dot{N}_6\,dx$$

$$k_{33}=\int_0^{l_e}\alpha_4\ddot{N}_3^2\,dx+\int_0^{l_e}\alpha_5\dot{N}_3^2\,dx,\quad k_{34}=\int_0^{l_e}\alpha_3\dot{N}_3N_4\,dx,\quad k_{35}=\int_0^{l_e}\alpha_4\ddot{N}_3\ddot{N}_5\,dx+\int_0^{l_e}\alpha_5\dot{N}_3\dot{N}_5\,dx$$

$$k_{36}=\int_0^{l_e}\alpha_4\ddot{N}_3\ddot{N}_6\,dx+\int_0^{l_e}\alpha_5\dot{N}_3\dot{N}_6\,dx,\quad k_{44}=\int_0^{l_e}\alpha_1\dot{N}_4^2\,dx+\int_0^{l_e}\alpha_2N_4^2\,dx,\quad k_{45}=\int_0^{l_e}\alpha_3N_4\dot{N}_5\,dx$$

$$k_{46}=\int_0^{l_e}\alpha_3N_4\dot{N}_6\,dx,\quad k_{55}=\int_0^{l_e}\alpha_4\ddot{N}_5^2\,dx+\int_0^{l_e}\alpha_5\dot{N}_5^2\,dx,\quad k_{56}=\int_0^{l_e}\alpha_4\ddot{N}_5\ddot{N}_6\,dx+\int_0^{l_e}\alpha_5\dot{N}_5\dot{N}_6\,dx$$

and

$$k_{66} = \int_0^{l_e} \alpha_4 \ddot{N}_6^2 \, dx + \int_0^{l_e} \alpha_5 \dot{N}_6^2 \, dx$$

where

$$\alpha_1 = (E_1A_1 + E_3A_3e^2), \quad \alpha_2 = \overline{G}bh_2\left(-\frac{(1+e)}{h_2}\right)^2, \quad \alpha_3 = \overline{G}bh_2\left(\frac{D}{h_2}\right)\left(-\frac{(1+e)}{h_2}\right)$$

$$\alpha_4 = (E_1I_1 + E_3I_3) \quad \text{and} \quad \alpha_5 = \overline{G}bh_2\left(\frac{D}{h_2}\right)^2$$

Mass matrix of the sandwich beam element comprising MR fluid within the mid-layer:

$$m_{11} = \int_0^{l_e} \beta_1 N_1^2 \, dx + \int_0^{l_e} \beta_2 N_1^2 \, dx, \quad m_{12} = \int_0^{l_e} \beta_3 N_1 \dot{N}_2 \, dx, \quad m_{13} = \int_0^{l_e} \beta_3 N_1 \dot{N}_3 \, dx$$

$$m_{14} = \int_0^{l_e} \beta_1 N_1 N_4 \, dx + \int_0^{l_e} \beta_4 N_1 N_4 \, dx, \quad m_{15} = \int_0^{l_e} \beta_3 N_1 \dot{N}_5 \, dx, \quad m_{16} = \int_0^{l_e} \beta_3 N_1 \dot{N}_6 \, dx$$

$$m_{22} = \int_0^{l_e} \beta_5 N_2^2 \, dx + \int_0^{l_e} \beta_6 \dot{N}_2^2 \, dx, \quad m_{23} = \int_0^{l_e} \beta_5 N_2 N_3 \, dx + \int_0^{l_e} \beta_6 \dot{N}_2 \dot{N}_3 \, dx, \quad m_{24} = \int_0^{l_e} \beta_3 N_4 \dot{N}_2 \, dx$$

$$m_{25} = \int_0^{l_e} \beta_5 N_2 N_5 \, dx + \int_0^{l_e} \beta_6 \dot{N}_2 \dot{N}_5 \, dx, \quad m_{26} = \int_0^{l_e} \beta_5 N_2 N_6 \, dx + \int_0^{l_e} \beta_6 \dot{N}_2 \dot{N}_6 \, dx$$

$$m_{33} = \int_0^{l_e} \beta_5 N_3^2 \, dx + \int_0^{l_e} \beta_6 \dot{N}_3^2 \, dx, \quad m_{34} = \int_0^{l_e} \beta_3 N_4 \dot{N}_3 \, dx$$

$$m_{35} = \int_0^{l_e} \beta_5 N_3 N_5 \, dx + \int_0^{l_e} \beta_6 \dot{N}_3 \dot{N}_5 \, dx \quad m_{36} = \int_0^{l_e} \beta_5 N_3 N_6 \, dx + \int_0^{l_e} \beta_6 \dot{N}_3 \dot{N}_6 \, dx$$

$$m_{44} = \int_0^{l_e} \beta_1 N_4^2 \, dx + \int_0^{l_e} \beta_4 N_4^2 \, dx, \quad m_{45} = \int_0^{l_e} \beta_3 N_4 \dot{N}_5 \, dx, \quad m_{46} = \int_0^{l_e} \beta_3 N_4 \dot{N}_6 \, dx$$

$$m_{55} = \int_0^{l_e} \beta_5 N_5^2 \, dx + \int_0^{l_e} \beta_6 \dot{N}_5^2 \, dx, \quad m_{56} = \int_0^{l_e} \beta_5 N_5 N_6 \, dx + \int_0^{l_e} \beta_6 \dot{N}_5 \dot{N}_6 \, dx$$

$$m_{66} = \int_0^{l_e} \beta_5 N_6^2 \, dx + \int_0^{l_e} \beta_6 \dot{N}_6^2 \, dx$$

where

$$\beta_1 = \rho_1A_1 + e^2\rho_3A_3, \quad \beta_2 = \rho_2I_2\left(-\frac{(1+e)}{h_2}\right)^2, \quad \beta_3 = (\rho_2I_2 + \rho_rI_r)\left(\frac{D}{h_2}\right)\left(-\frac{(1+e)}{h_2}\right)$$

$$\beta_4 = (\rho_2I_2 + \rho_rI_r)\left(\frac{(1+e)}{h_2}\right)^2, \quad \beta_5 = (\rho_1A_1 + \rho_2A_2 + \rho_rA_r + \rho_3A_3)$$

$$\beta_6 = (\rho_2I_2 + \rho_rI_r)\left(\frac{D}{h_2}\right)^2$$

References

[1] X.Q. He, T.Y. Ng, S. Sivasahankar, K.M. Liew, Active control of FGM plates with integrated piezoelectric sensors and actuators, *International Journal of Solids and Structures* 38 (2001) 1641–1655.

[2] M.J. Lam, D.J. Inman, W.R. Saunders, Vibration control through passive constrained layer damping and active control, *Journal of Intelligent Materials and Structures* 8 (1997) 663–677.

[3] Y. Gu, R.L. Clark, C.L. Fuller, A.C. Zander, Experiments on active control of plate vibration using piezoelectric actuators and polyvinylidene fluoride (PWDF) modal sensors, *Journal of Vibration and Acoustics* 116 (1994) 303–308.

[4] B.F. Spencer Jr., S. Nagarajaiah, State of the art of structural control, *Journal of Structural Engineering* 129 (2003) 845–856.

[5] Y.L. Xu, W.L. Qu, J.M. Ko, Seismic response control of frame structures using magnetorheological/electrorheological dampers, *Earthquake Engineering and Structural Dynamics* 29 (2000) 557–575.

[6] R. Stanway, J.L. Sproston, A.K. El Wahed, Applications of electrorheological fluids in vibration control: a survey, *Smart Materials and Structures* 5 (1996) 464–482.

[7] G.Z. Yao, F.F. Yap, G. Chen, W.H. Li, S.H. Yeo, MR damper and its application for semi-active control of vehicle suspension system, *Mechatronics* 12 (2002) 963–973.
[8] H.U. Oh, J. Onoda, An experimental study of a semi-active magneto-rheological fluid variable damper for vibration suppression of truss structures, *Smart Materials and Structures* 11 (2002) 156–162.
[9] T. Pranoto, K. Nagaya, A. Hosoda, Vibration suppression of plate using linear MR fluid passive damper, *Journal of Sound and Vibration* 276 (2004) 919–932.
[10] K.D. Weiss, J.D. Carlson, D.A. Nixon, Viscoelastic properties of magneto- and electro-rheological fluids, *Journal of Intelligent Materials and Structures* 5 (1994) 772–775.
[11] J. Wang, G. Meng, Magnetorheological fluid devices: principles, characteristics and applications in mechanical engineering, *Proceedings of Institution of Mechanical Engineers Part L: Journal of Materials* 215 (2001) 165–174.
[12] J.D. Carlson, K.D. Weiss, A growing attraction to magnetic fluids, *Machine Design* 66 (1994) 61–64.
[13] S.J. Dyke, B.F. Spencer, M.K. Sain, J.D. Calrson, An experimental study of MR dampers on seismic protection, *Smart Materials and Structures* 7 (1998) 693–703.
[14] S.B. Choi, Vibration control of flexible structures using ER dampers, *Journal of Dynamic Systems, Measurement and Control, Transaction of ASME* 121 (1999) 134–138.
[15] Z.G. Ying, W.Q. Zhu, A stochastic optimal semi-active control strategy for ER/MR dampers, *Journal of Sound and Vibration* 259 (2003) 45–62.
[16] G.J. Hiemenz, N.M. Wereley, Seismic response of civil structures utilizing semi-active MR and ER bracing systems, *Journal of Intelligent Materials and Structures* 10 (1999) 646–651.
[17] M.V. Gandhi, B.S. Thomson, S.B. Choi, A new generation of innovative ultra-advanced intelligent composite materials featuring electro-rheological fluids: an experimental investigation, *Journal of Composite Materials* 23 (1989) 1232–1255.
[18] Y. Choi, A.F. Sprecher, H. Conrad, Vibration characteristics of a composite beam containing an electrorheological fluid, *Journal of Intelligent Materials and Structures* 1 (1990) 91–104.
[19] M. Yalcintas, J.P. Coulter, Analytical modeling of electrorheological materials based adaptive beams, *Journal of Intelligent Materials and Structures* 6 (1995) 488–497.
[20] M. Yalcintas, J.P. Coulter, Electrorheological materials based non-homogeneous adaptive beams, *Smart Materials and Structures* 7 (1998) 128–143.
[21] M. Yalcintas, H. Dai, Magnetorheological and electrorheological materials in adaptive structures and their performance comparison, *Smart Materials and Structures* 8 (1999) 560–573.
[22] M. Yalcintas, H. Dai, Vibration suppression capabilities of magneto-rheological materials based adaptive structures, *Smart Materials and Structures* 13 (2004) 1–11.
[23] Q. Sun, J.X. Zhou, L. Zhang, An adaptive beam model and dynamic characteristics of magnetorheological materials, *Journal of Sound and Vibration* 261 (2003) 465–481.
[24] Z.F. Yeh, Y.S. Shih, Dynamic characteristics and dynamic instability of magnetorheological based adaptive beams, *Journal of Composite Materials* 40 (2006) 1333–1359.
[25] R.A. DiTaranto, Theory of vibratory bending of elastic and viscoelastic layered finite-length beams, *Journal of Applied Mechanics, Transactions of ASME, Series E* 87 (1965) 881–886.
[26] V. Rajamohan, R. Sedaghati, S. Rakheja, Vibration analysis of a multi-layer beam containing magnetorheological fluid, *Smart Materials and Structures* 19 (2010) 015013 12pp.
[27] G. Haiqing, L.M. King, T.B. Cher, Influence of a locally applied electrorheological fluid layer on vibration of a simple cantilever beam, *Journal of Intelligent Materials and Structures* 4 (1993) 379–384.
[28] G. Haiqing, L.M. King, Vibration characteristics of sandwich beams partially and fully treated with electrorheological fluid, *Journal of Intelligent Materials and Structures* 8 (1997) 401–413.
[29] D.J. Mead, S. Markus, The forced vibration of a three-layer, damped sandwich beam with arbitrary boundary conditions, *Journal of Sound and Vibration* 10 (1969) 163–175.
[30] W.H. Li, G. Chen, S. Yeo, Viscoelastic properties of MR fluids, *Smart Materials and Structures* 8 (1999) 460–468.
[31] Y.T. Choi, J.U. Cho, S.B. Choi, N.M. Wereley, Constitutive models of electrorheological and magnetorheological fluids using viscometers, *Smart Materials and Structures* 14 (2005) 1025–1036.
[32] F.D. Goncalves, J.H. Koo, M. Ahmadian, A review of the state of the art in magnetorheological fluid technologies—part I: MR fluid and MR fluid models, *The Shock and Vibration Digest* 38 (2006) 203–219.
[33] S.S. Rao, *The Finite Element Method in Engineering*, Butterworth Heinemann, Boston, 1999.